

Inactivation of Capicua drives cancer metastasis

Ross A. Okimoto, Frank Breitenbuecher, Victor R. Olivas, Wei Wu, Beatrice Gini, Matan Hofree, Saurabh Asthana, Gorjan Hrustanovic, Jennifer Flanagan, Asmin Tulpule, Collin M. Blakely, Henry J. Haringsma, Andrew D. Simmons, Kyle Gowen, James Suh, Vincent A. Miller, Siraj Ali, Martin Schuler, Trever G. Bivona

The supplemental data includes 15 figures and legends, primer sequences, and four supplemental tables. Supplemental table 1 is provided here, while supplemental tables 2, 3a, 3b, and 4 are provided as separate excel files.

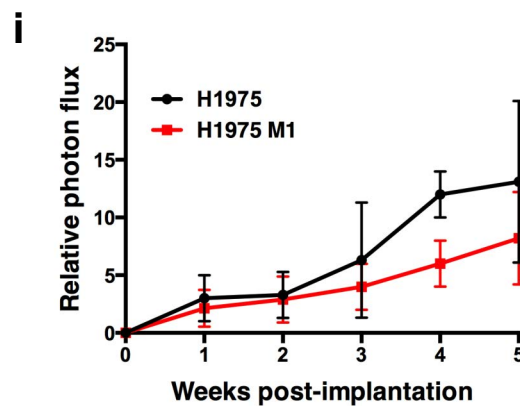
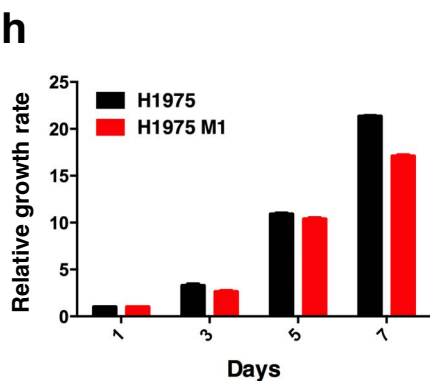
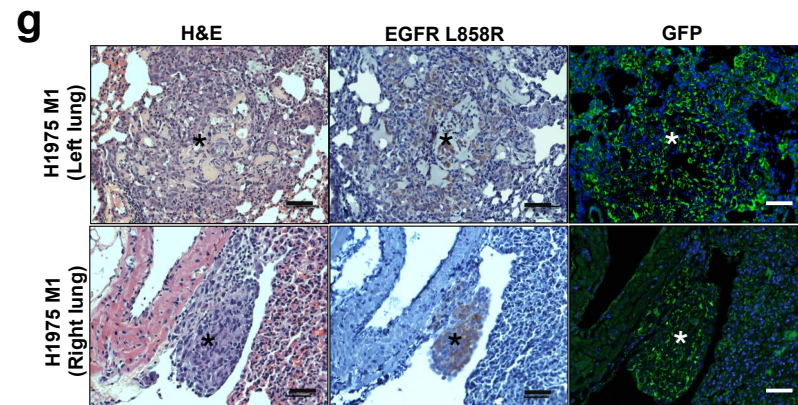
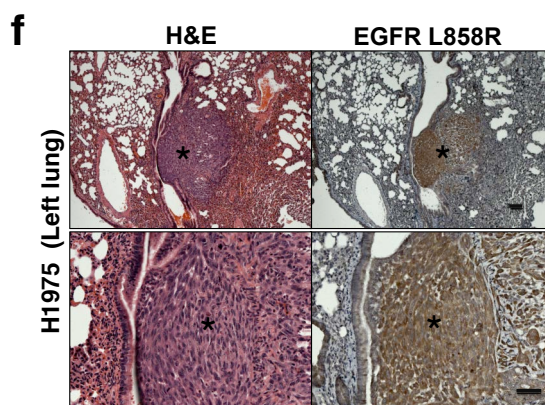
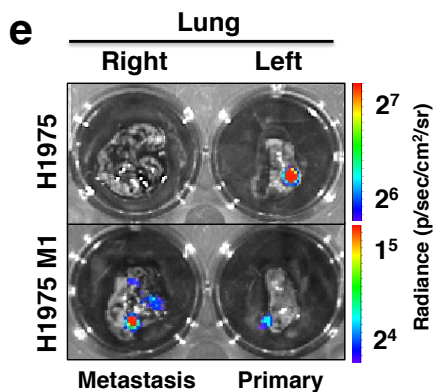
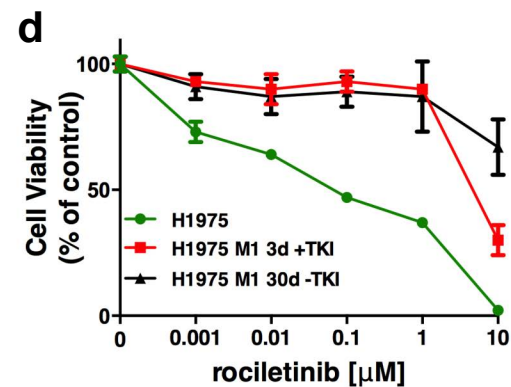
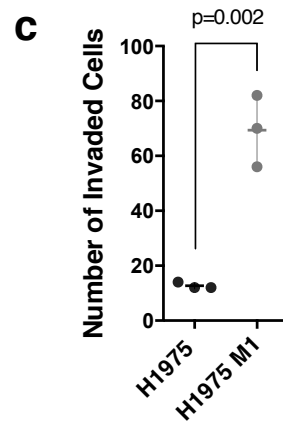
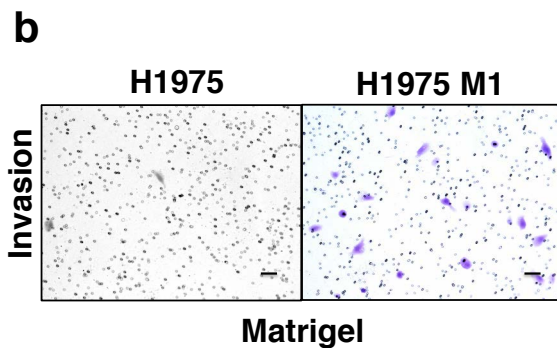
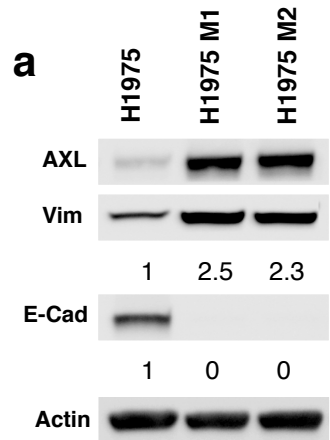


Figure S1. Development of an *in vivo* orthotopic lung cancer metastasis model.

(a) Immunoblots for epithelial (E-Cadherin) and mesenchymal (Vimentin and AXL) markers in H1975, H1975 M1 and M2. (b) Invasion of H1975 and H1975 M1 cells. Scale bars, 100 μm . (c) Number of cells invaded through Matrigel. Results of two independent experiments in triplicate are shown. p-value, Student's t-test; error bars represent SEM. (d) Cell viability of H1975, H1975 M1 continuously treated with rociletinib, and H1975 M1 grown in the absence of rociletinib for 30 days then treated with rociletinib for 3 days prior to CTG assay. Performed in triplicate. Error bars represent SEM. (e) Representative *ex vivo* BLI of the right and left lung of H1975 and H1975 M1 mice. (f) H&E and EGFR L858R IHC staining of an orthotopically implanted primary (left) lung tumor from a mouse bearing H1975 cells. Scale bars, 100 μm (top panels) and 50 μm (bottom panels). *Tumor. (g) H&E, EGFR L858R, and GFP staining of an orthotopically implanted primary lung tumor (left lung) and metastasis (right lung) from a mouse bearing H1975 M1 cells. Scale bar, 50 μm . *Tumor. (h) *In vitro* growth rate comparing H1975 and H1975 M1 cells by CTG assay, relative to day 1. Performed in triplicate. Error bars represent SEM. (i) Normalized mean photon flux over 5 weeks in mice bearing H1975 or H1975 M1 cells. Error bars represent SEM.

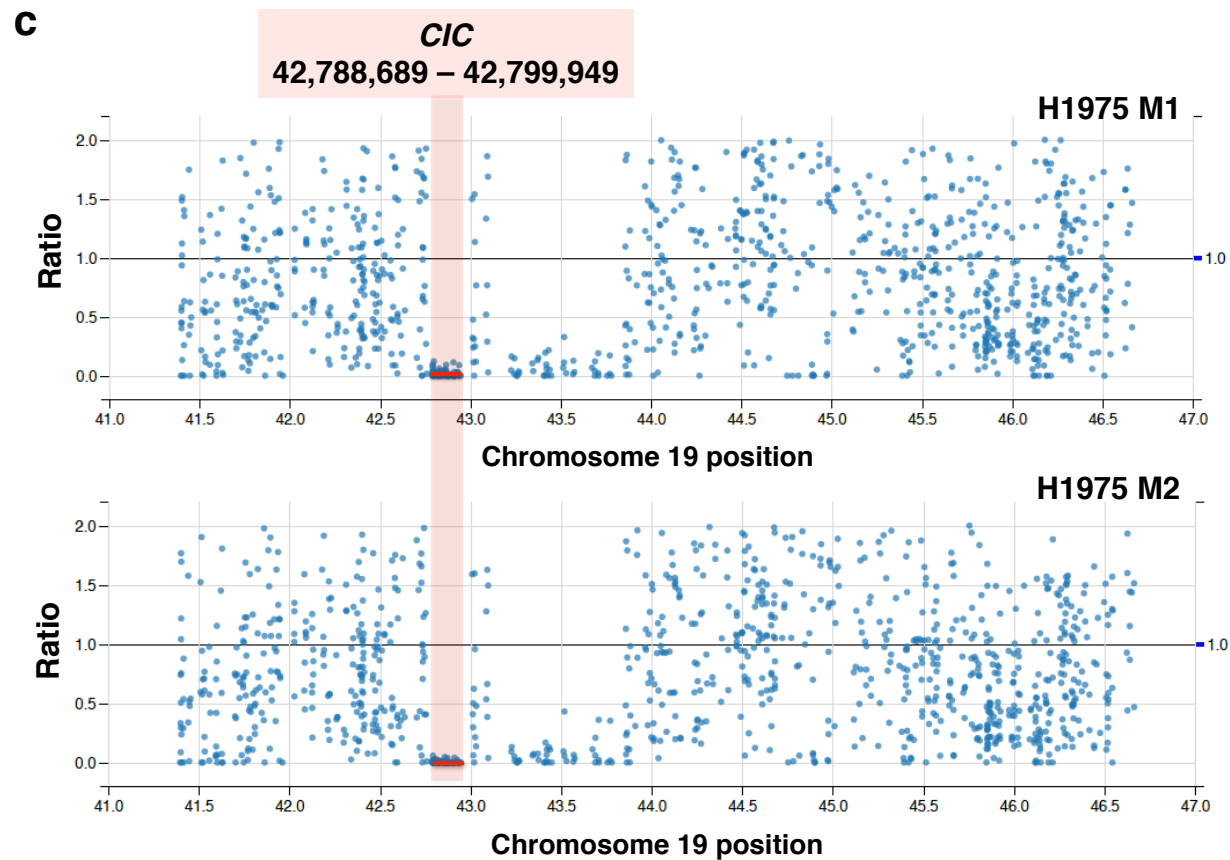
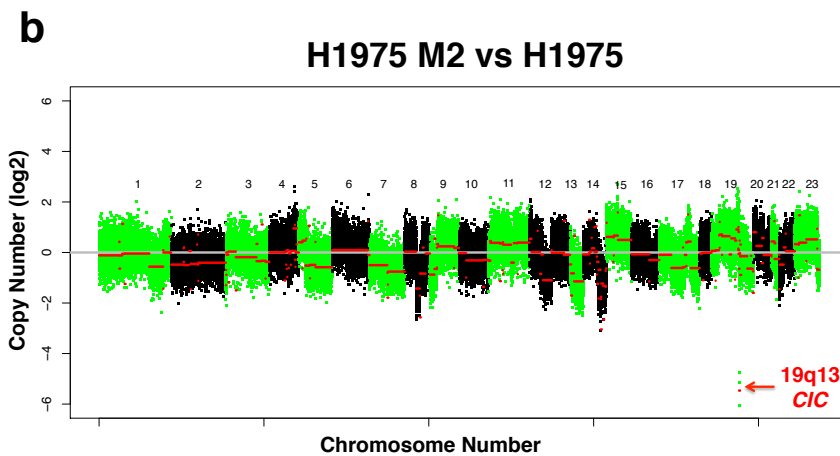
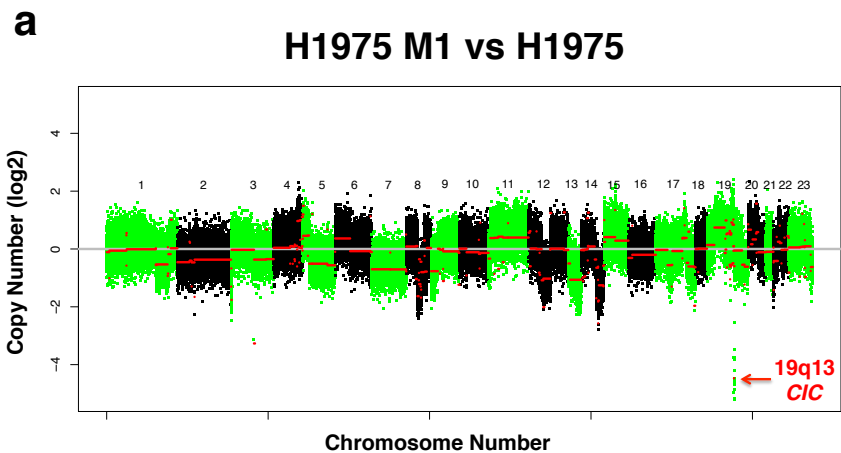


Figure S2. Copy number analysis identifies a focal deletion in hypermetastatic lung cancer cells. (a-b) Whole exome CNV profile comparing H1975 M1 (a) and H1975 M2 (b) to parental H1975 cells. (c) Predicted copy number alterations from exome sequencing analysis at the CIC locus (Chromosome 19 position 42,772,689 – 42,799,949 in human GRCH37/hg19) in H1975 M1 and H1975 M2 using Control-FREEC ratios and the Shiny application. The CN ratio (y-axis) between tumor DNA (H1975 M1 or H1975 M2 cells) and normal germline DNA at the genomic region containing CIC (highlighted in the pink) is depicted. Mean CN ratio demarcated with red horizontal line. Chromosome 19 coordinates are indicated on the x-axis.

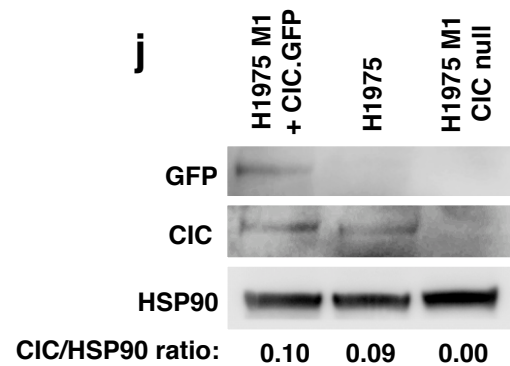
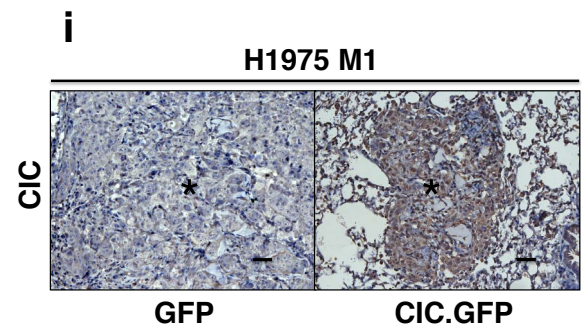
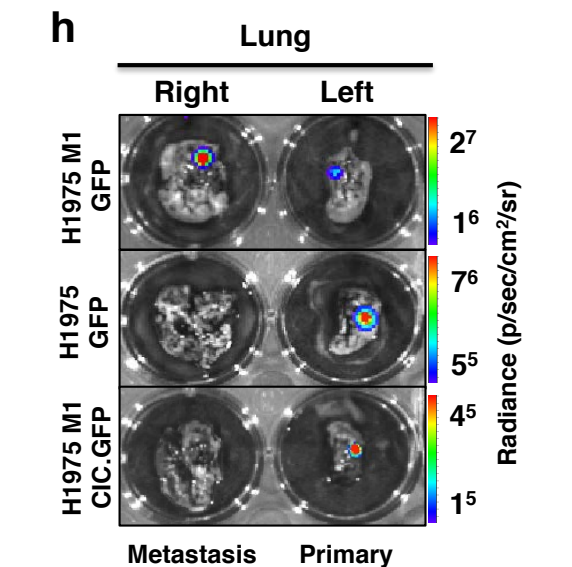
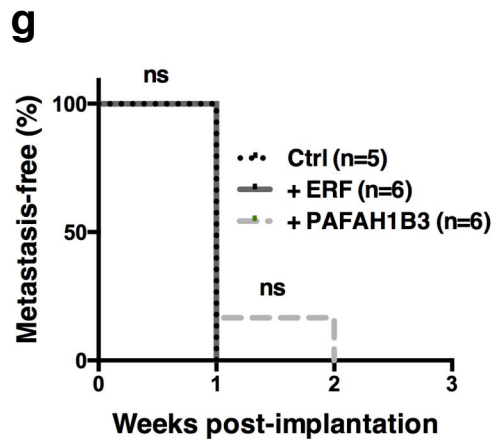
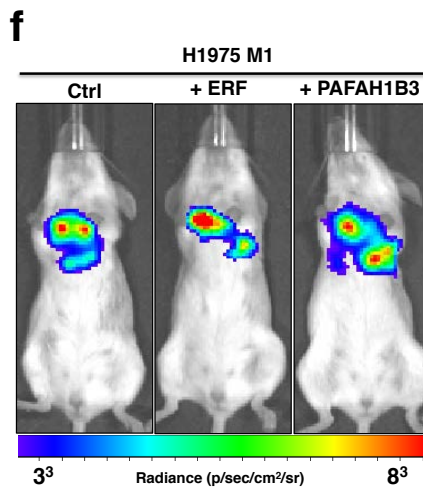
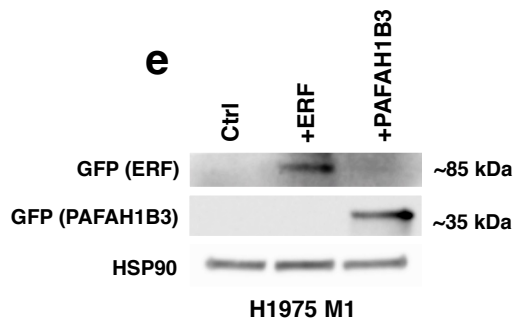
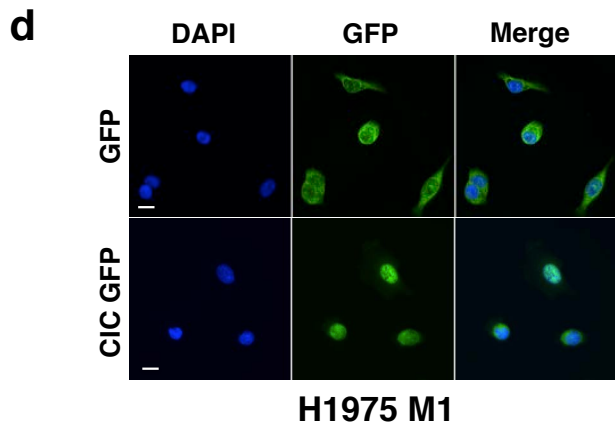
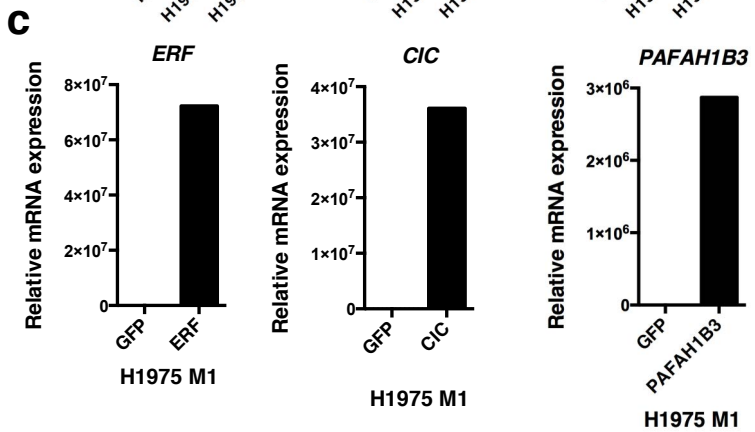
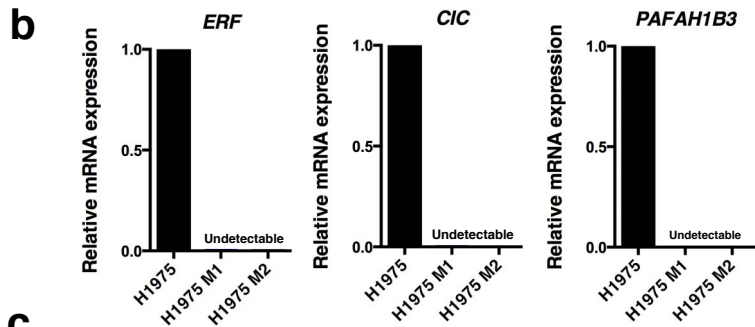
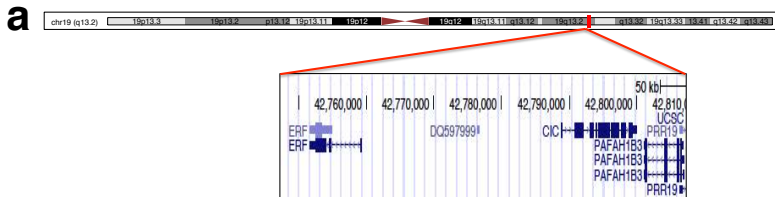


Figure S3. In vivo orthotopic model identifies CIC as a metastasis suppressor. (a) Region of genomic loss on chromosome 19. (b) Relative ERF, CIC, PAFAH1B3 mRNA expression from RNAseq analysis between H1975 and H1975 M1 or M2. (c) Relative ERF, CIC, PAFAH1B3 mRNA expression by qRT-PCR in H1975 and H1975 M1 cells following genetic reconstitution. Results of two independent experiments in triplicate are shown. Error bars represent SEM. (d) H1975 M1 cells expressing either GFP control or GFP-tagged CIC. DAPI = blue, GFP = green. Experiments were performed in triplicate with a total of 9 high-power fields (HPFs) imaged from the GFP (control) and 9 HPFs from the CIC.GFP groups. All cells expressing GFP-tagged CIC demonstrated nuclear GFP staining. Scale bars, 20 μ m. (e) Immunoblot of H1975 M1 cells expressing either luciferase control, GFP-tagged ERF, or GFP-tagged PAFAH1B3. (f) BLI images of mice bearing H1975 M1 cells expressing either luciferase control, GFP-tagged ERF, or GFP-tagged PAFAH1B3. (g) Metastasis-free survival of luciferase control (n=5), GFP-tagged ERF (n=6), or GFP-tagged PAFAH1B3 (n=6) expressing H1975 M1 mice in (f). Representative ex vivo BLI of the right and left lungs of H1975 M1 GFP-Luc, H1975 GFP-Luc, or H1975 M1 cells expressing GFP-tagged CIC. (i) CIC staining of orthotopically implanted tumors from H1975 M1 mice expressing either GFP-Luc or GFP-tagged CIC. Scale bars, 50 μ m. (j) Immunoblot of H1975 M1 cells with reconstituted CIC.GFP compared to H1975 endogenous CIC and H1975 M1 (CIC null). Representative of two independent experiments.

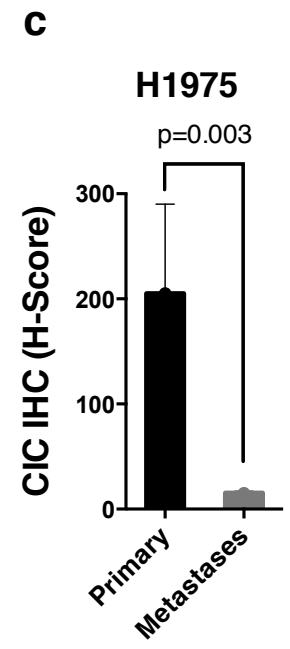
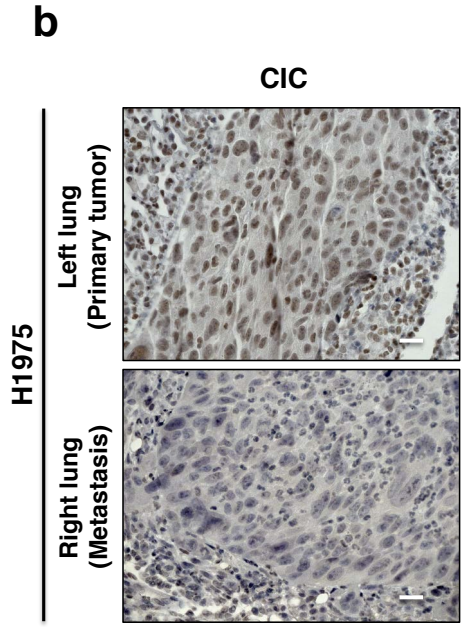
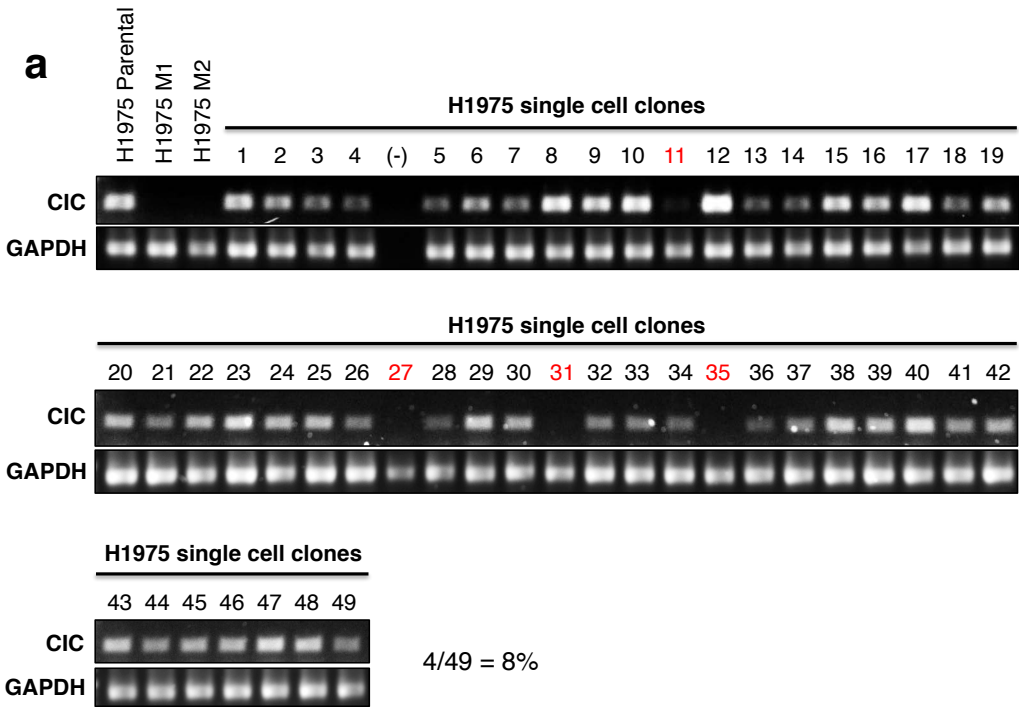
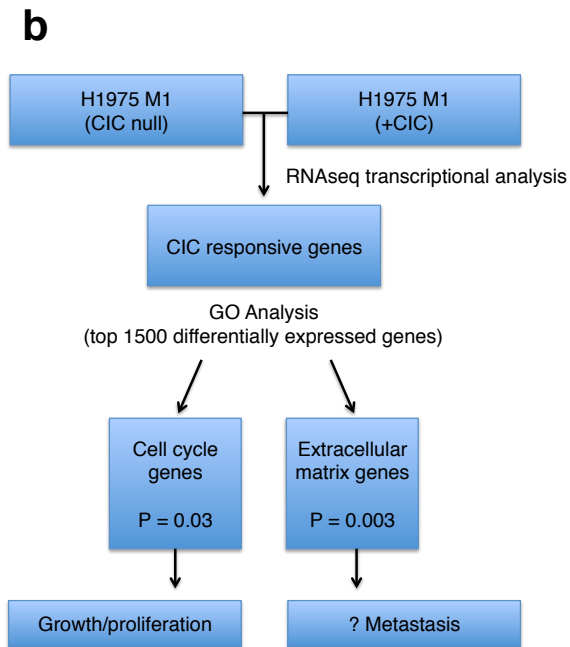
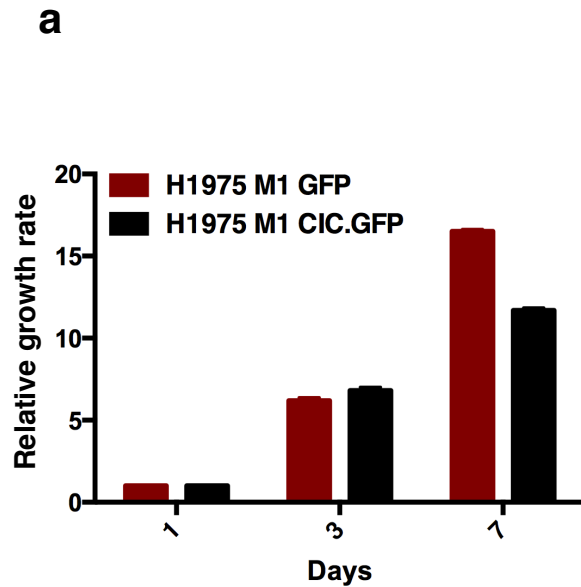


Figure S4. Decreased CIC expression correlates with metastasis. (a) Genomic PCR amplification (exon four and flanking introns) of *CIC* in H1975, H1975 M1, H1975 M2, and 49 H1975 single cell derived subclones. (b) Representative IHC images of the primary tumor and paired metastasis from a H1975 mouse that developed metastasis. Scale bar, 20 μ m. (c) Nuclear CIC IHC scoring of primary tumors and metastasis derived from the H1975 mice who developed metastasis (n=3 total mice). p-value, student's t-test. Error bars represent SEM.



c

Downregulated CIC responsive cell cycle genes

GENE	FOLD CHANGE	ADJUSTED P-VALUE
CCNB2	0.71	1.31E-31
CCNA1	0.61	3.96E-28
CCNG2	0.66	1.09E-26
CCNB1	0.77	2.19E-18
CCNI	0.79	2.30E-17
CCNG1	0.70	4.91E-15
CDC25C	0.70	5.64E-22
CDCA2	0.75	3.03E-21
CDC40	0.81	7.31E-12
ANAPC15	0.64	5.41E-40
ANAPC16	0.75	8.73E-22

Figure S5. A subset of CIC responsive genes regulates the cell cycle in lung cancer cells. (a) In vitro growth rate comparing H1975 M1 GFP and H1975 M1 CIC.GFP cells by CTG assay, relative to day 1. Performed in triplicate. Error bars represent SEM. (b) Algorithm to identify and functionally cluster CIC responsive genes. (c) Downregulated CIC responsive cell cycle genes.

Proteinaceous extracellular matrix

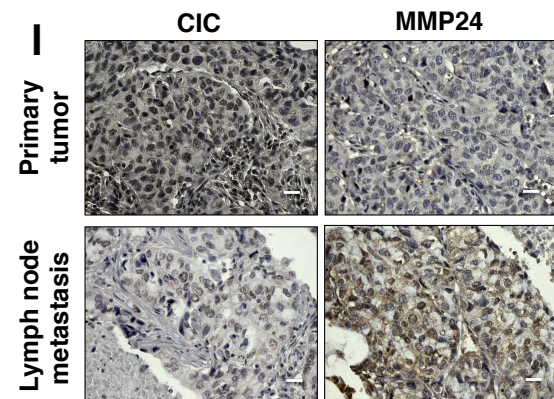
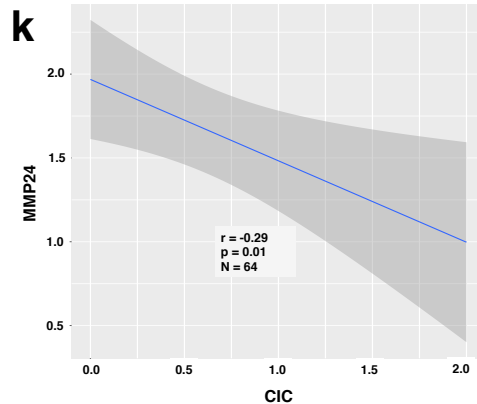
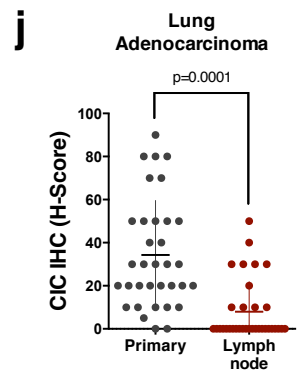
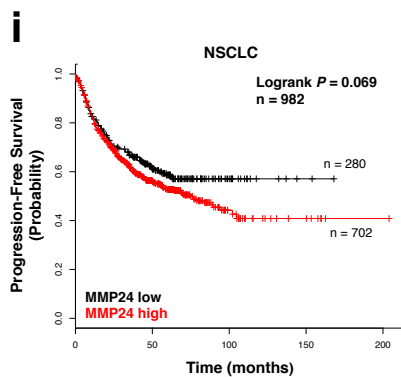
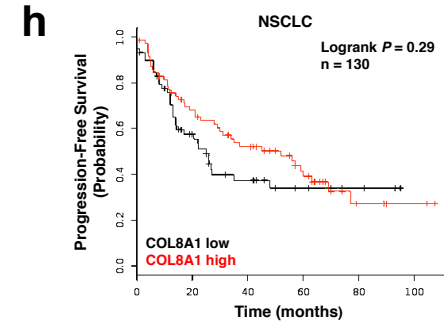
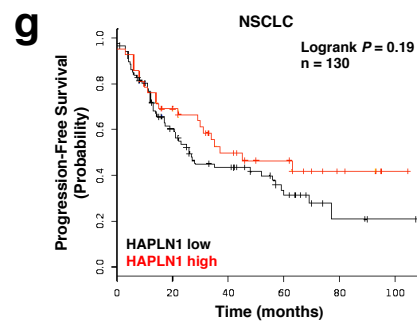
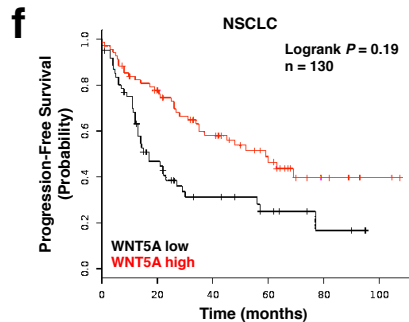
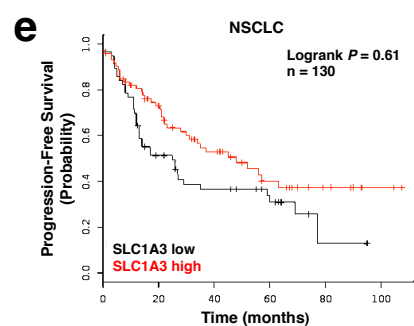
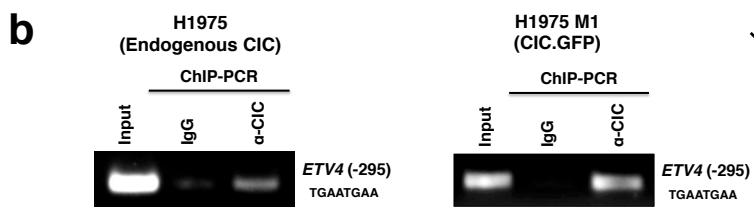
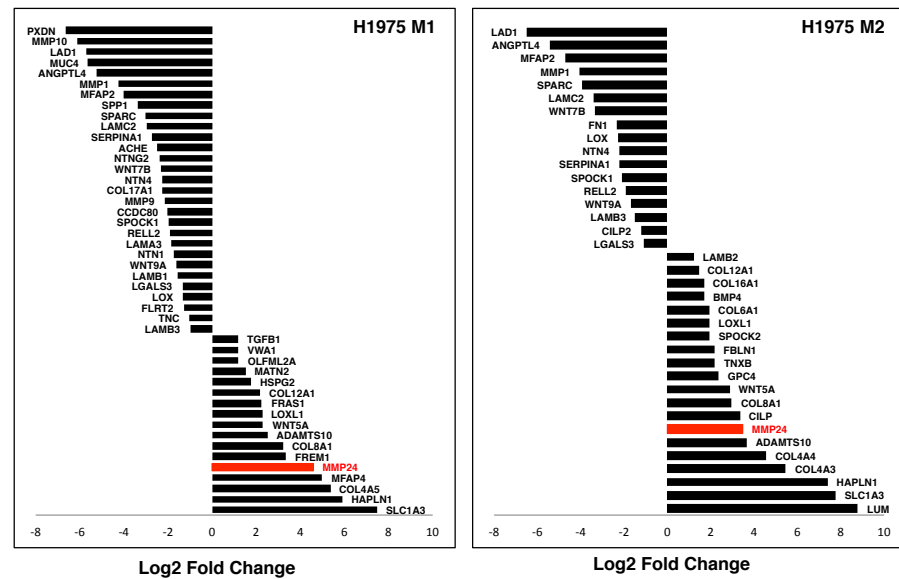
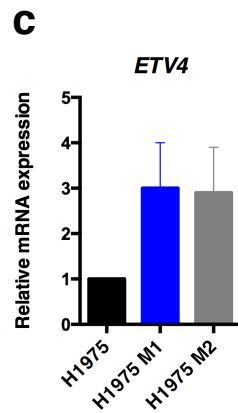
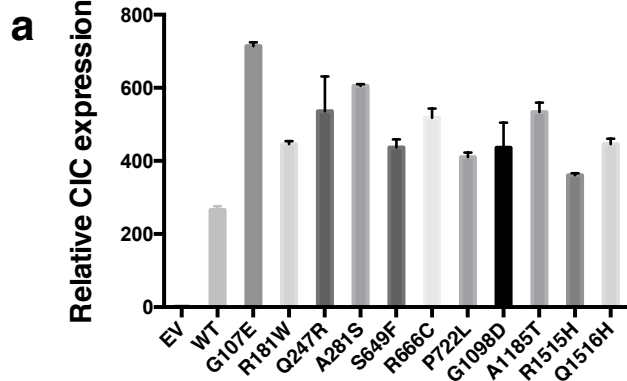


Figure S6. Identification of MMP24 as a metastasis effector downstream of CIC.

(a) Relative CIC protein expression from WT and CIC mutants. Obtained from two independent experiments. Error bars, SEM. (b) ChIP-PCR in H1975 and H1975 M1 CIC.GFP expressing cells. Representative of two independent experiments. (c) Relative ETV4 mRNA expression in H1975, H1975 M1, and H1975 M2 cells. Representative of two independent experiments and performed in triplicate. Error bars, SEM. (d) Differential expression of Proteinaceous ECM genes between H1975 versus H1975 M1 or H1975 M2. (e-h) PFS for patients with LN positive (N1) NSCLC with either high or low *SLC1A3* mRNA expression. n=130; p=0.61. Probe 202800_at. (e), high or low *WNT5A* mRNA expression. n=130; p=0.19. Probe 213425_at. (f), high or low *HAPLN1* mRNA expression. n=130; p=0.19. Probe 205523_at. (g), high or low *COL8A1* mRNA expression. n=130; p=0.29. Probe 214587_at. (h). (i) PFS for NSCLC patients with either *MMP24* high or *MMP24* low mRNA expression. n=982, p=0.069. Probe 213171_s_at. (j) CIC score of matched primary lung tumors and LN metastases. Mean +/- SEM, 33 +/- 4.3 (normal, n=32) and 7.1 +/- 2.3 (tumor, n=32). p value, Student's t-test. (k) Correlation between CIC and MMP24 protein expression (r = -0.29, p=0.01, n=64). (l) MMP24 and CIC staining of primary and LN metastasis. Scale bar, 20 μ m.

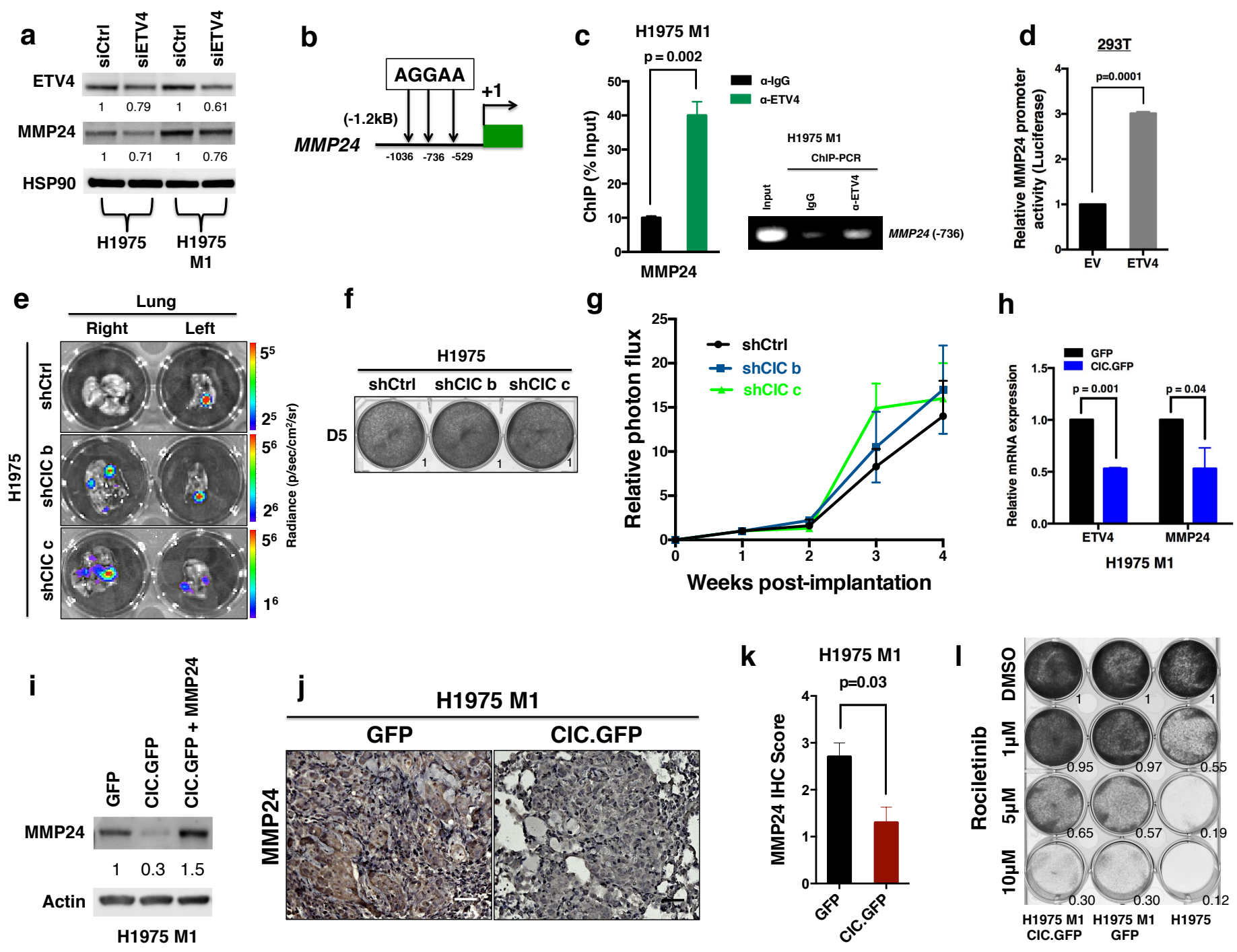


Figure S7. MMP24 is a metastasis effector downstream of CIC.

(a) Immunoblot comparing ETV4 and MMP24 expression with siETV4 or control (siCtrl).
(b) *MMP24* promoter region. (c) ChIP-PCR in H1975 M1 cells demonstrating *MMP24* promoter occupancy by ETV4. p-value, Student's t-test. Error bars, SEM. Representative of two independent experiments. (d) Relative *MMP24* luciferase promoter activity with ETV4 overexpression compared to empty vector. p value, Student's t-test. Error bars represent SEM, n=5. (e) *Ex vivo* BLI of lungs from mice bearing H1975 cells expressing either shCtrl, shCIC b, or shCIC c. (f) CV assay comparing H1975 shCtrl, shCICb, or shCICc expressing cells. Representative of 2 independent experiments. (g) Relative photon flux comparing mice bearing H1975 cells expressing either shCtrl, shCIC b, or shCIC c. (h) *ETV4* and *MMP24* qRT-PCR in H1975 M1 cells expressing GFP or GFP-tagged CIC. Results of two independent experiments in triplicate are shown. p value, Student's t-test. Error bars represent SEM. (i) Immunoblot of H1975 M1 cells with GFP, CIC.GFP, or CIC.GFP +MMP24. Representative of two independent experiments. (j) *MMP24* staining of orthotopic tumors from H1975 M1 mice expressing either GFP-Luc or GFP-tagged CIC. Scale bars, 50 μ m. (k) Mean *MMP24* IHC score from orthotopically implanted tumors bearing GFP control (n = 3) or CIC.GFP (n = 3). p-value, Student's t-test. Error bars, SEM. (l) CV assay of H1975, H1975 M1, or H1975 M1 cells expressing GFP-tagged CIC +/- rociletinib treatment. Representative of 2 independent experiments.

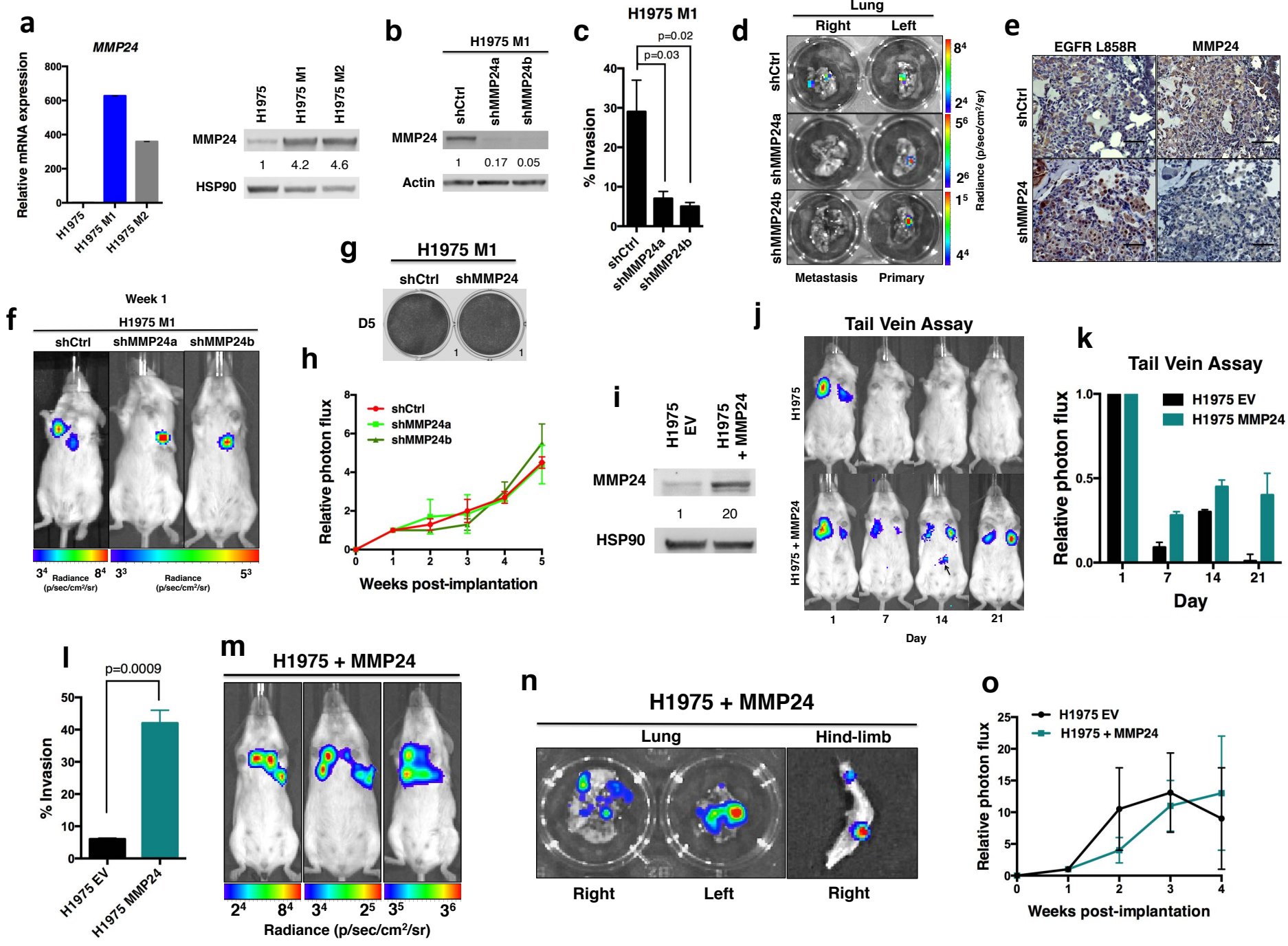


Figure S8. CIC effector, MMP24, is a multistep mediator of lung cancer metastasis.

(a) MMP24 qRT-PCR and immunoblot from H1975, H1975 M1, and M2. qRT-PCR results obtained from two independent experiments in triplicate. Error bars, SEM. (b) Immunoblots for H1975 M1 shCtrl, shMMP24a, or shMMP24b. (c) H1975 M1 shCtrl, shMMP24a, or shMMP24b invasion. Results of two independent experiments in triplicate. p-value, Student's t-test. Error bars, SEM. (d) *Ex vivo* BLI of lungs from shCtrl, shMMP24a, or shMMP24b H1975 M1 GFP-Luc mice. (e) EGFR^{L858R} and MMP24 staining of lung tumors from H1975 M1 shCtrl and shMMP24a. Scale bars, 50 μ m. (f) BLI of shCtrl, shMMP24a, or shMMP24b H1975 M1 GFP-Luc mice one week post-implantation. (g) CV of shCtrl or shMMP24 H1975 M1 cells. Results representative of 2 independent experiments. (h) Normalized mean photon flux from H1975 M1 shCtrl, shMMP24a and shMMP24b mice over 5 weeks. Error bars, SEM. (i) MMP24 Immunoblot from H1975 +EV or +MMP24. (j) Tail vein assay comparing H1975 GFP-Luc (n=4) and H1975 GFP-luc +MMP24 (n=4) mice. Arrow (luciferin injection site). (k) Relative photon flux (normalized to day 1) of H1975 GFP-Luc (n=4) and H1975 GFP-Luc +MMP24 (n=4) cohorts. (l) Invasion of H1975 cells +EV or +MMP24. p-value, Student's t-test. Error bars, SEM. (m) BLI of mice bearing H1975 GFP-Luc +MMP24 cells. (n) *Ex vivo* BLI of right and left lungs and right hindlimb of a H1975 mouse overexpressing MMP24. (o) Normalized mean photon flux of H1975 EV and H1975 +MMP24 mice over 4 weeks. Error bars, SEM.

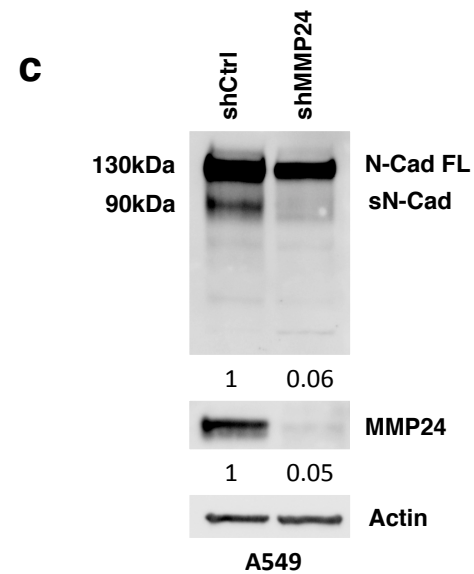
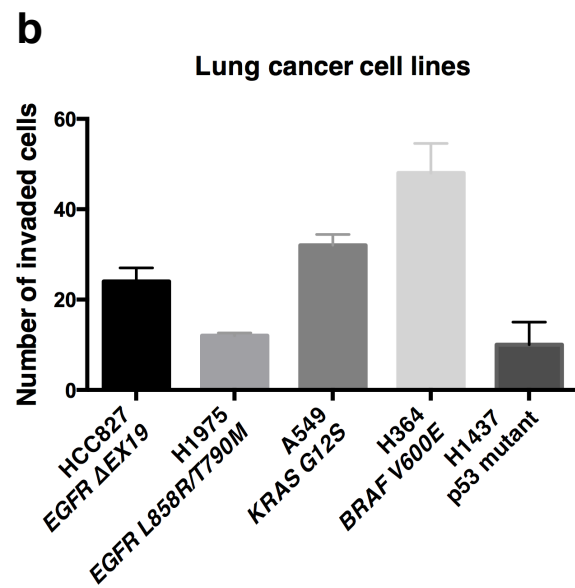
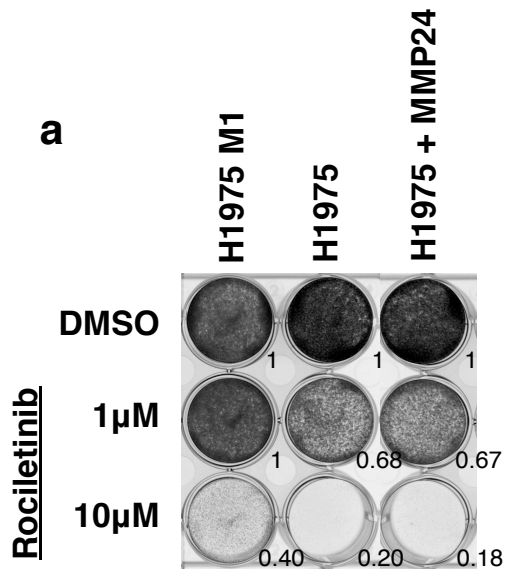
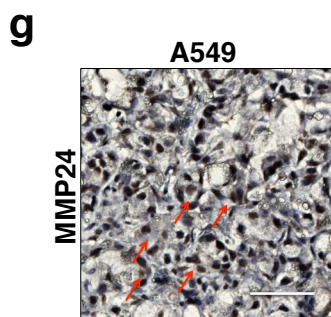
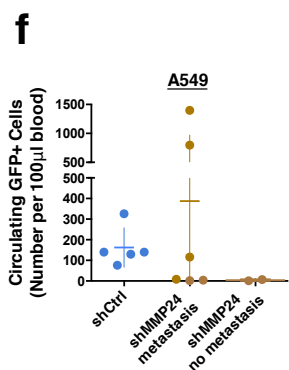
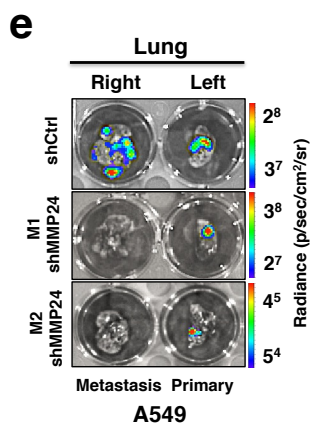
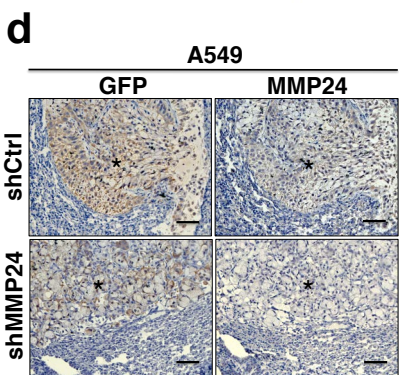
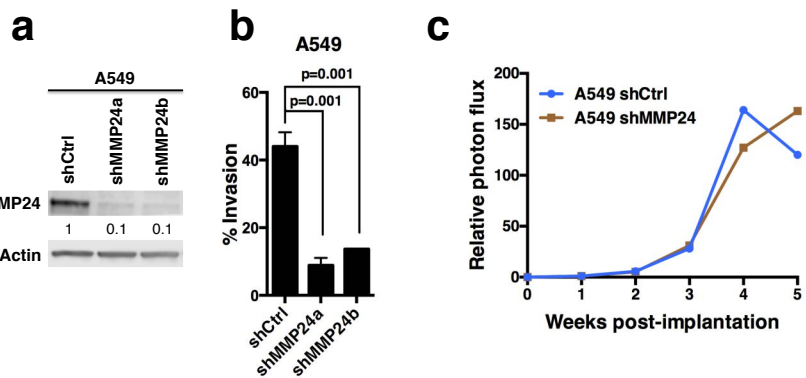


Figure S9. MMP24 correlates with increased invasion in treatment naïve lung cancer cells. (a) Crystal violet assay of H1975 M1, H1975, and H1975 +MMP24 +/- rociletinib. Results representative of 2 independent experiments. (b) Bar graph depicting the number of cells invaded cells in a panel of lung cancer cell lines. Error bars, SEM. (c) Immunoblots for N-Cadherin in A549 MMP24 KD cells compared to shCtrl. FL = full length and S = soluble.

A549



HCC364

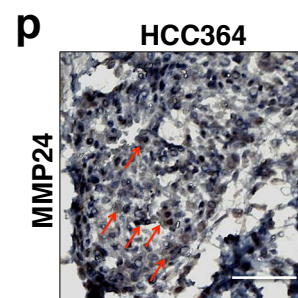
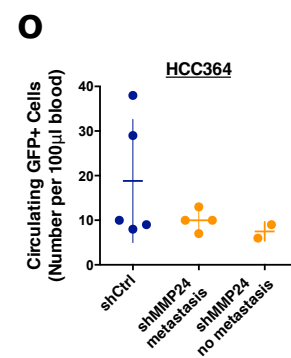
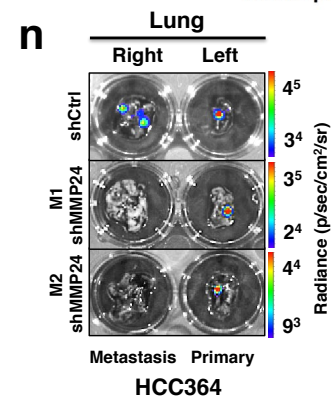
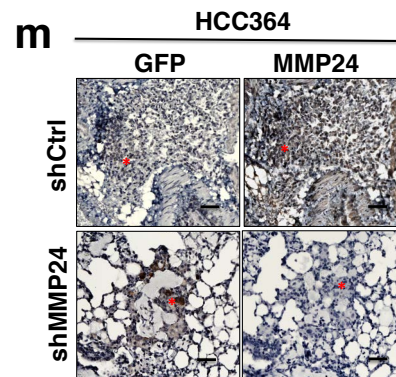
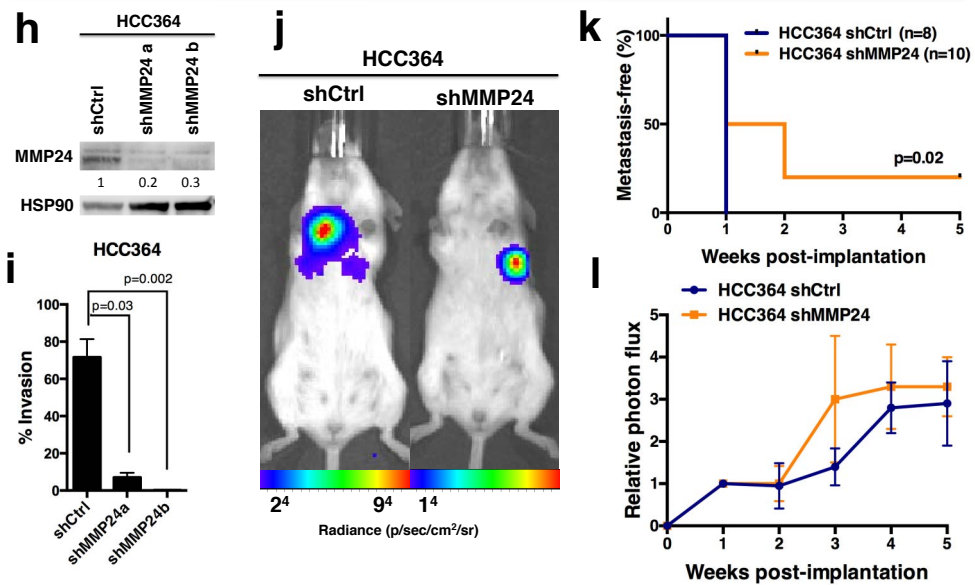
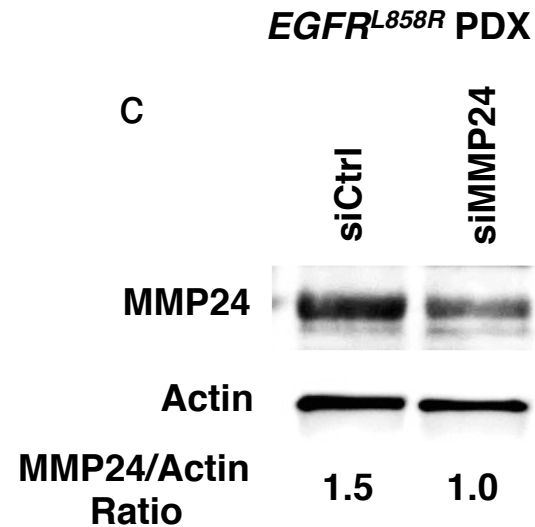
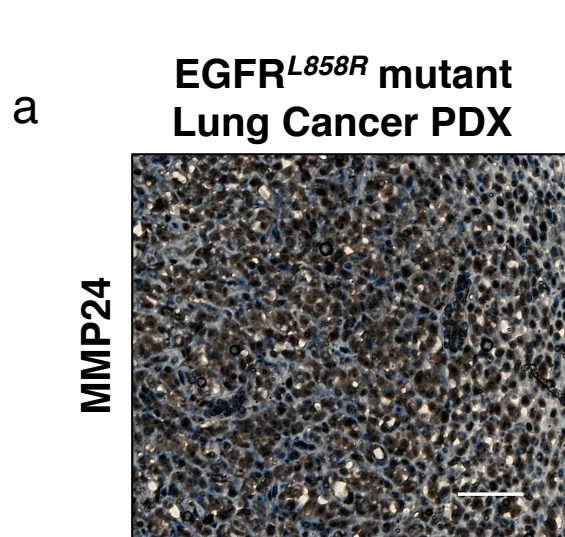


Figure S10. MMP24 promotes metastasis across molecular subsets. (a) Immunoblot for shCtrl, shMMP24a, and shMMP24b A549 cells. (b) A549 invasion with shCtrl, shMMP24a, or shMMP24b. Two independent experiments in triplicate. p-value, Student's t-test. Error bars, SEM. (c) Normalized mean photon flux of shCtrl and shMMP24a A549 mice over 5 weeks. Error bars, SEM. (d) MMP24 staining of A549 shCtrl and shMMP24 tumors. Scale bars, 50 μ m. (e) *Ex vivo* BLI of lungs from A549 shCtrl and non-metastatic shMMP24a mice. (f) Circulating GFP+ cells/100 μ l of blood at 5 weeks post-implantation. Mean \pm SEM, 162 \pm 42 (shCtrl, n=5), 387 \pm 238 (shMMP24 metastasis, n=6), 4 \pm 3 (shMMP24 no metastasis, n=2). (g) MMP24+ tumor cells (arrows) in a shMMP24 A549 mouse with metastasis. (h) Immunoblots for shCtrl, shMMP24a, and shMMP24b HCC364 cells. (i) HCC364 invasion with shCtrl, shMMP24a, or shMMP24b. Two independent experiments in triplicate. p-value, Student's t-test. Error bars, SEM. (j) BLI of shCtrl or shMMP24a HCC364 GFP-Luc mice. (k) Metastasis-free survival comparing HCC364 shCtrl and shMMP24a mice; p values, log-rank. (l) Normalized mean photon flux of HCC364 shCtrl and shMMP24a mice over 5 weeks. Error bars, SEM. (m) MMP24 staining of HCC364 shCtrl or shMMP24 tumors. Scale bars, 50 μ m. (n) *Ex vivo* BLI of lungs from HCC364 shCtrl and non-metastatic shMMP24a mice (o) Circulating GFP+ cells/100 μ l of blood at 5 weeks post-implantation. Mean \pm SEM, 19 \pm 6.0 (shCtrl, n=5), 10 \pm 1.2 (shMMP24 metastasis, n=4), 7.5 \pm 1.5 (shMMP24 no metastasis, n=2). Error bars, SEM. (p) MMP24+ tumor cells (arrows) in a shMMP24 HCC364 mouse with metastasis.



b

Score	Expect	Identities	Gaps	Strand	Frame
291 bits(157)	2e-82()	159/160(99%)	0/160(0%)	Plus/Plus	

Features:

Query	2468	AGGGCATGAACTACTTGGAGGACCGTCGCTTGGTGCACCGCGACCTGGCAGCCAGGAACG	2527		
Sbjct	42	AGGGCATGAACTACTTGGAGGACCGTCGCTTGGTGCACCGCGACCTGGCAGCCAGGAACG	101		
Query	2528	TACTGGTGAAAACACCGCAGCATGTCAAGATCACAGATTTTGGGCTGGCCAAACTGCTGG	2587	EGFR CDS	
Sbjct	102	TACTGGTGAAAACACCGCAGCATGTCAAGATCACAGATTTTGGGCGGGCCAAACTGCTGG	161	EGFR PDX	
Query	2588	GTGCGGAAGAGAAAAGAATACCATGCAGAAGGAGGCAAAGT	2627	2573 T>G_EGFR L858R	
Sbjct	162	GTGCGGAAGAGAAAAGAATACCATGCAGAAGGAGGCAAAGT	201		

Figure S11. MMP24 is necessary for invasion in an EGFR^{L858R} PDX model.

(a) MMP24 IHC staining of an explanted EGFR^{L858R} PDX tumor. Scale bar, 50 μ m. (b) EGFR exon 21 sequence alignment comparing tumor DNA derived from the EGFR^{L858R} PDX sphere culture to wildtype EGFR sequence. (c) Immunoblot comparing MMP24 knockdown to control in the EGFR^{L858R} PDX derived sphere culture cells.

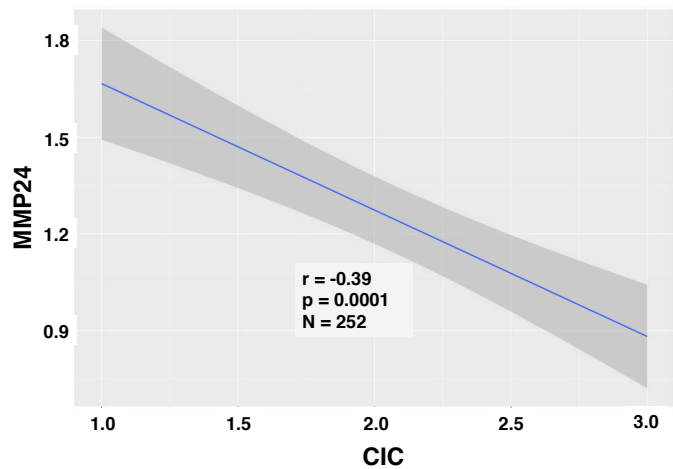
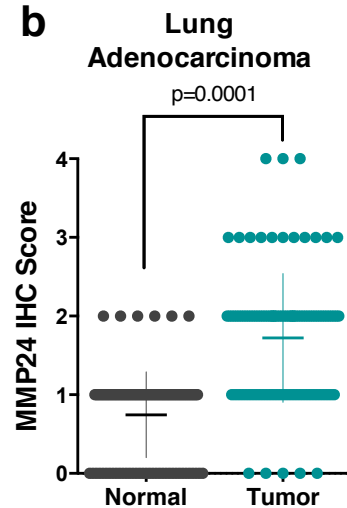
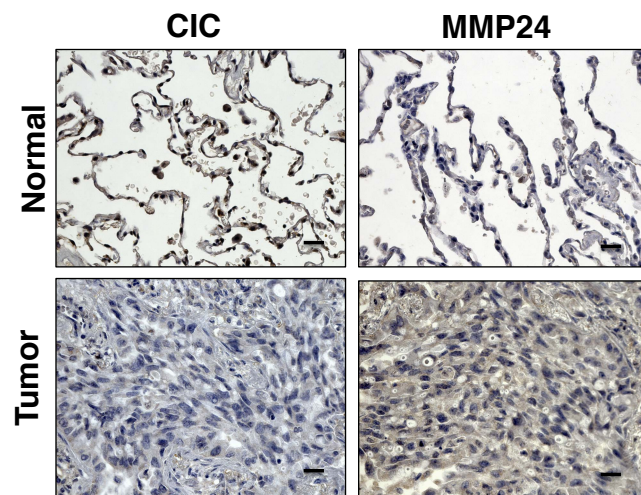
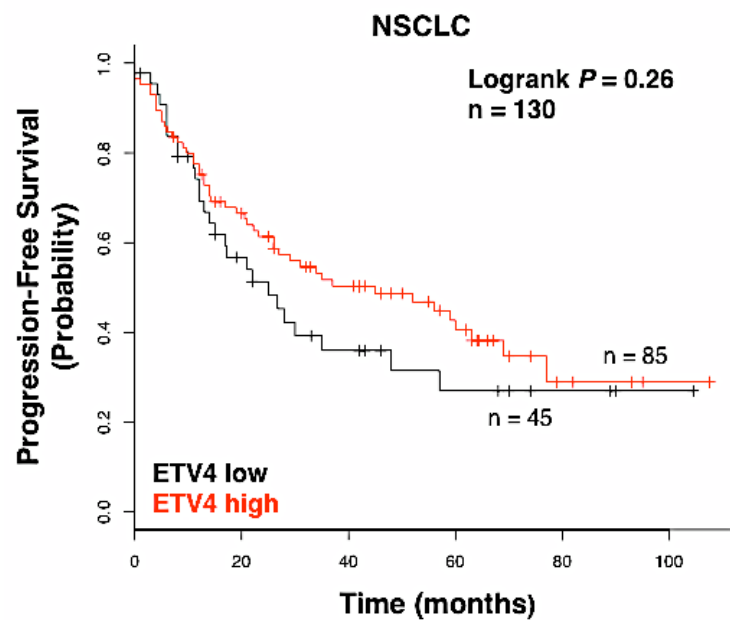
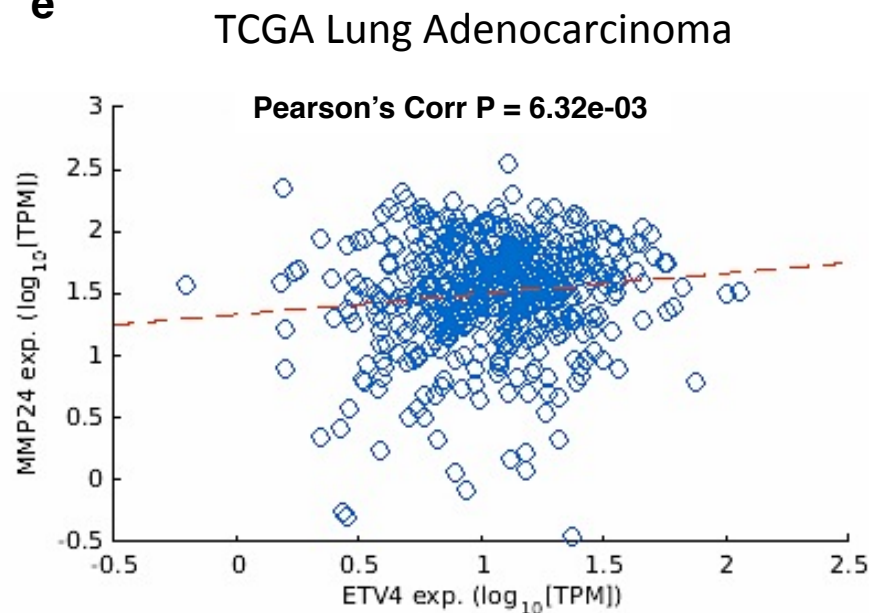
a**b****c****d****e**

Figure S12. Decreased CIC expression in lung adenocarcinoma correlates with increased MMP24 expression. (a) Correlation plot between CIC and MMP24 protein expression from lung adenocarcinoma tumors and adjacent normal tissue ($r = -0.39$, $p=0.0001$, $n=252$). (b) MMP24 staining in lung adenocarcinoma tumor specimens ($n = 130$) compared to normal adjacent tissue ($n = 126$). Mean \pm SEM, 0.75 ± 0.05 (normal, $n=126$) and 1.73 ± 0.08 (tumor, $n=130$). p -value, Student's t -test. (c) Representative images of MMP24 and CIC stained tissue sections of lung adenocarcinoma tissue and normal adjacent tissue. Scale bar, $20 \mu\text{m}$. (d) PFS for NSCLC patients with AJCC N1 disease with either *ETV4* high or *ETV4* low mRNA expression. $n=130$, $p=0.26$. Probe 211603_s_at. (e) Correlation plot between *ETV4* and MMP24 mRNA expression from the lung adenocarcinoma TCGA dataset ($n=275$).

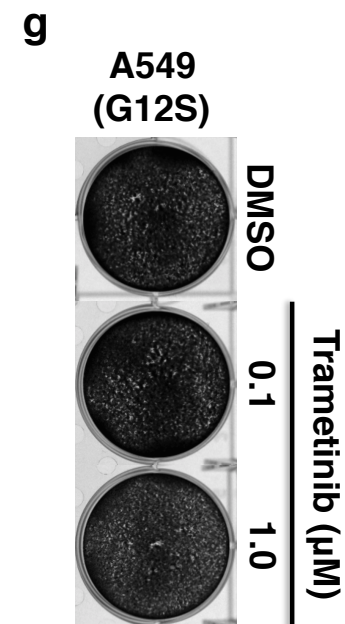
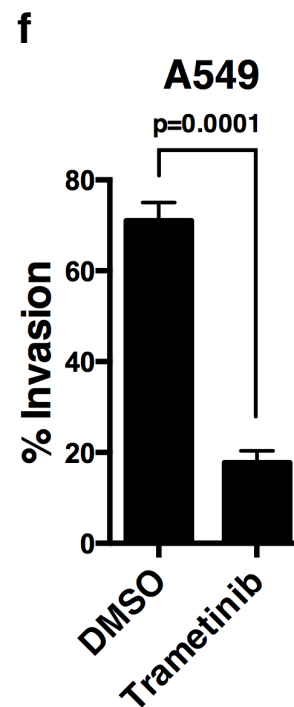
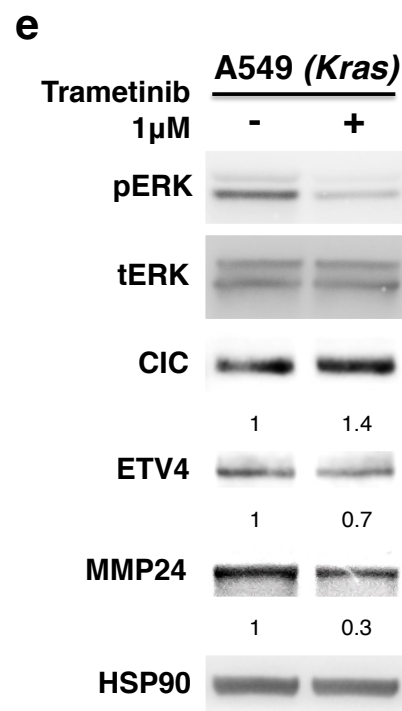
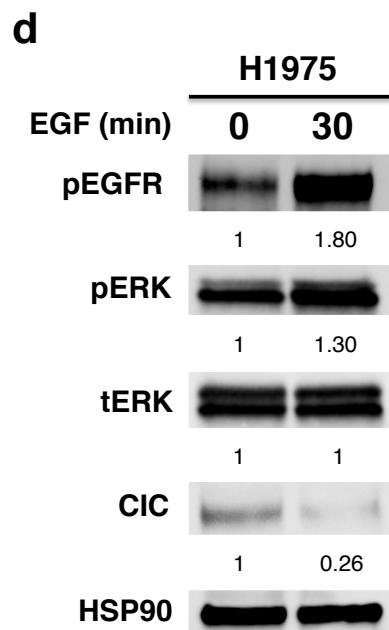
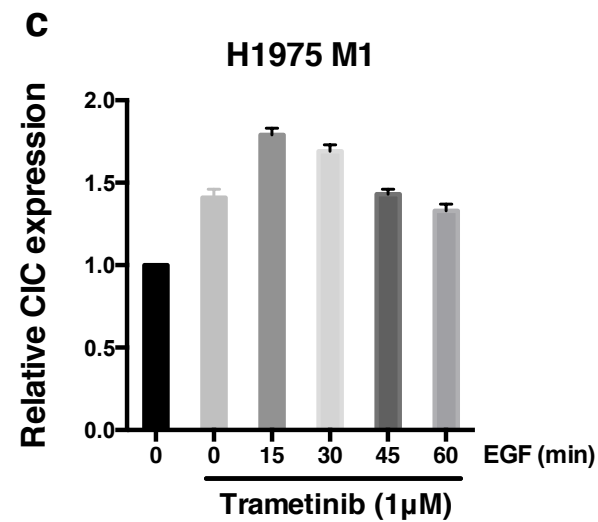
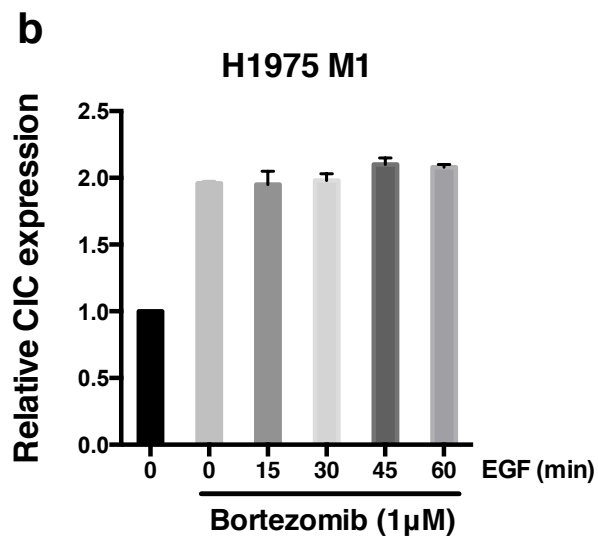
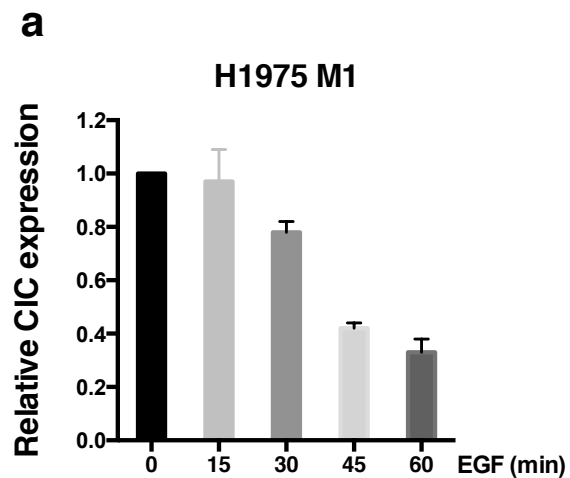
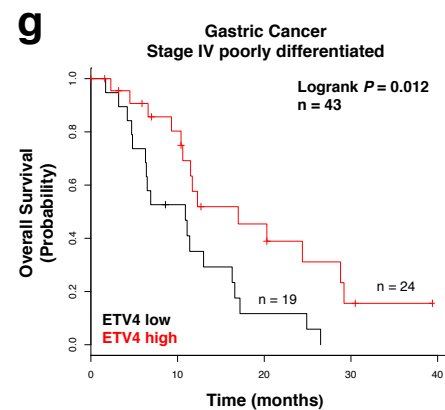
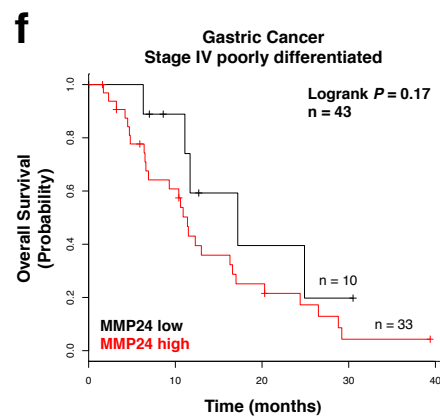
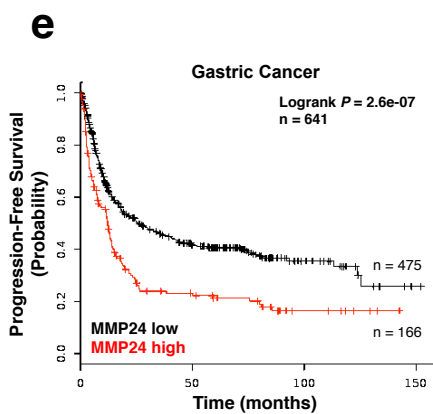
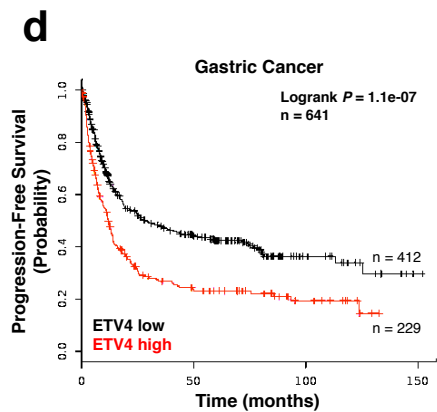
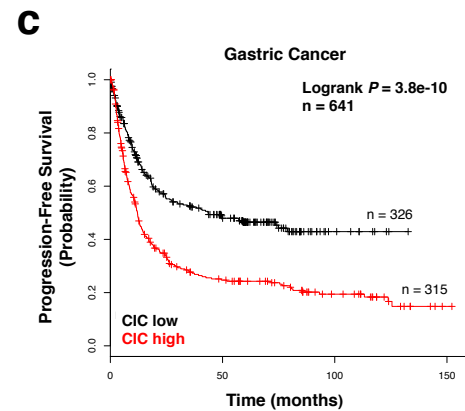
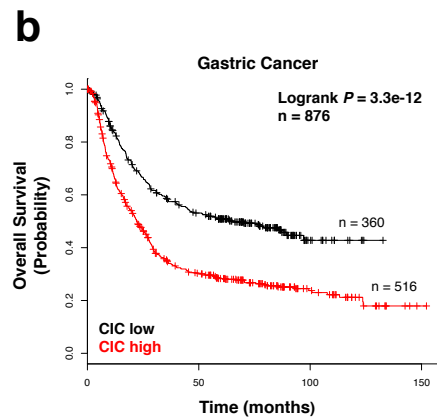
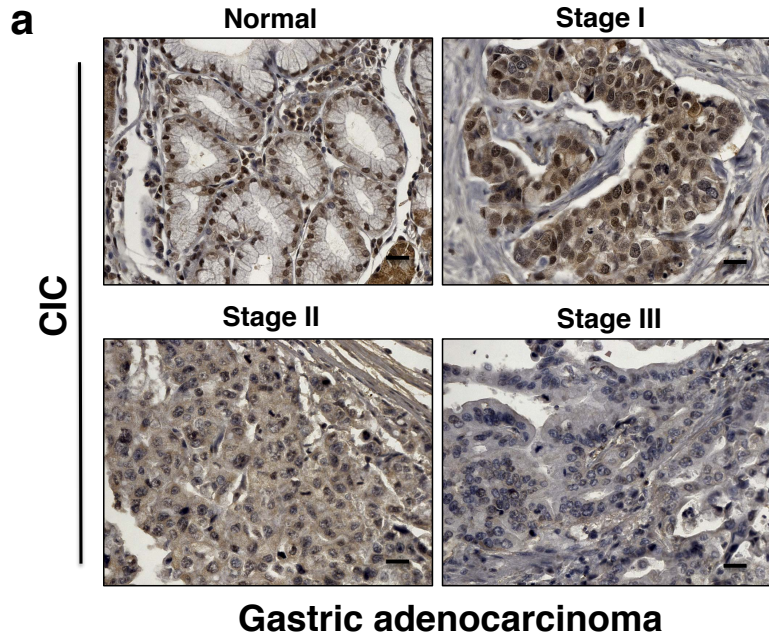


Figure S13. MAPK pathway regulates CIC expression. (a) Bar graph representing relative CIC protein expression in response to EGF stimulation over 60 minutes. Data obtained from two independent experiments (quantified with ImageJ). Error bars represent SEM. (b) Bar graph representing relative CIC protein expression in H1975 M1 cells pre-treated with Bortezomib and stimulated with EGF over 60 minutes. Data obtained from two independent experiments (quantified with ImageJ). Error bars represent SEM. (c) Bar graph representing relative CIC protein expression in H1975 M1 cells pre-treated with Trametinib and stimulated with EGF over 60 minutes. Data obtained from two independent experiments (quantified with ImageJ). Error bars represent SEM. (d) Immunoblot of phospho-ERK and endogenous CIC expression in H1975 cells after serum starvation and EGF stimulation for 30 minutes. Representative of two independent experiments. (e) Immunoblot comparing CIC, ETV4, and MMP24 expression in Trametinib treated A549 cells. Representative of two independent experiments. (f) Invasion comparing DMSO and Trametinib treated A549 cells. Representative of two independent experiments performed in triplicate. (g) Crystal violet viability assay comparing A549 cells treated with DMSO and Trametinib 0.1 μ M, and Trametinib 1.0 μ M. Representative of two independent experiments.



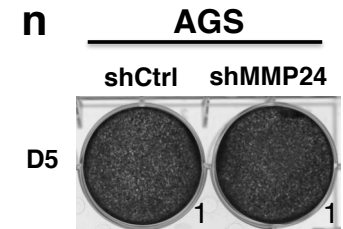
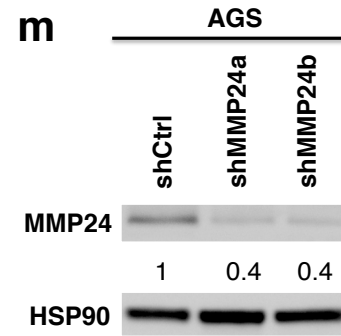
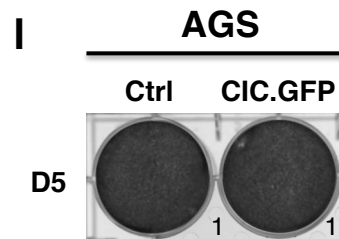
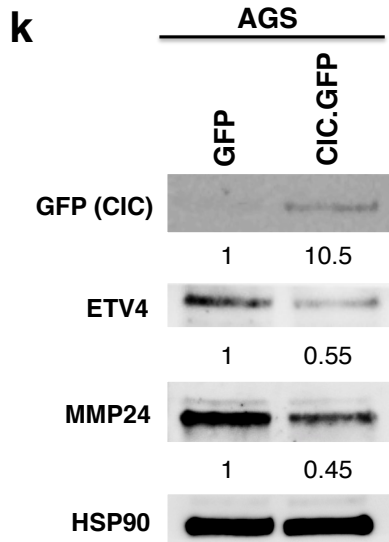
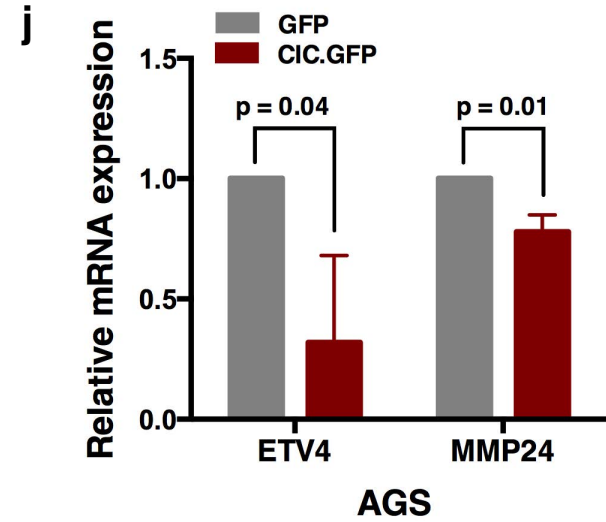
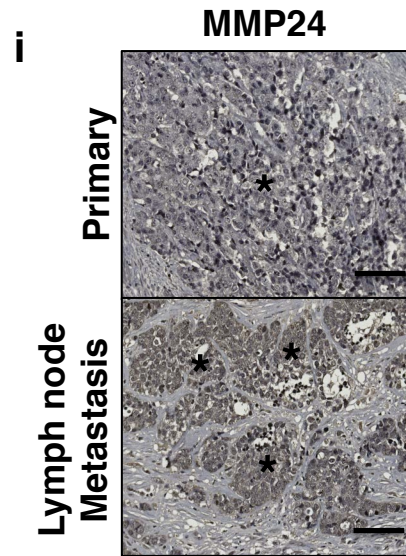
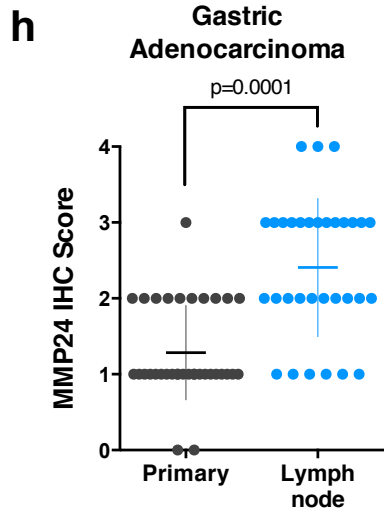


Figure S14. CIC effectors ETV4 and MMP24 enhance invasion and correlate with poor patient outcomes in gastric cancer. (a) Nuclear CIC staining in gastric adenocarcinoma by stage (I-III). Scale bar, 20 μ m. (b) OS for gastric cancer patients with either *CIC* high or *CIC* low mRNA expression. n=876, p=3.3e-12. Probe 212784_s_at. (c) PFS for gastric cancer patients with either *CIC* high or *CIC* low mRNA expression. n=641, p=3.8e-10. Probe 212784_s_at. (d-e) PFS for gastric cancer patients with either *ETV4* high or *ETV4* low mRNA expression. n=641, p=1.1e-07. Probe 211603_s_at. (d), *MMP24* high or *MMP24* low mRNA expression. n = 641, p = 2.6e-07. Probe 213171_s_at. (e). (f-g) OS for stage IV poorly differentiated gastric cancer patients with either *MMP24* high or *MMP24* low mRNA expression. n=43, p=0.17. Probe 213171_s_at. (f), *ETV4* high or *ETV4* low mRNA expression. n=43, p=0.012. Probe 211603_s_at. (g). (h) *MMP24* staining in primary GA tumors and LN metastases. Mean \pm SEM, 1.3 \pm 0.1 (primary, n=27) and 2.4 \pm 0.2 (LN metastasis, n=27). p-value, Student's t-test; error bars, SEM. (i) *MMP24* staining of primary and LN metastasis. Scale bar, 50 μ m. *Tumor. (j) *ETV4* and *MMP24* mRNA expression in GFP or GFP-tagged CIC AGS cells. Results of two independent experiments in triplicate. Error bars, SEM. (k) Immunoblots of AGS GFP and CIC-GFP cells. (l) CV assay of GFP or CIC-GFP AGS cells. Results representative of 2 independent experiments. (m) Immunoblots for AGS shCtrl, shMMP24a, shMMP24b. Representative of 2 independent experiments. (n) CV assay of shCtrl or shMMP24a AGS cells. Results representative of 2 independent experiments.

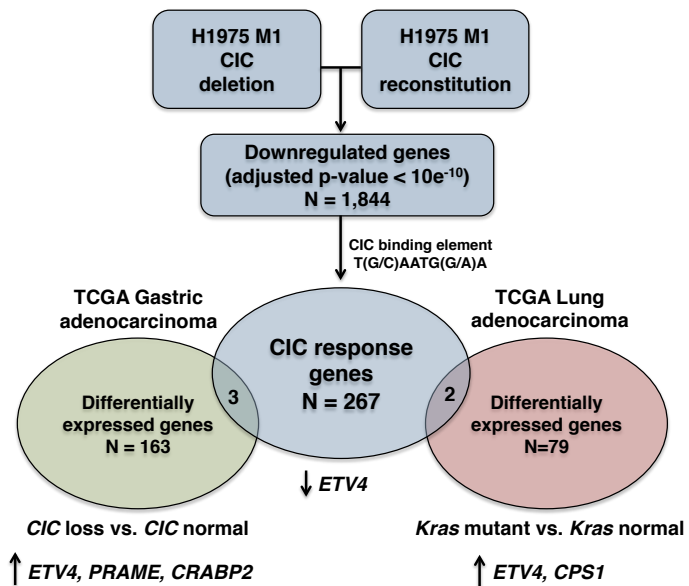
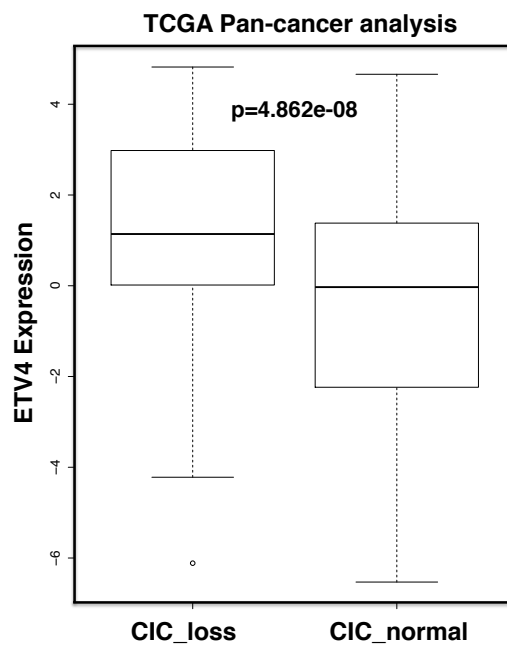
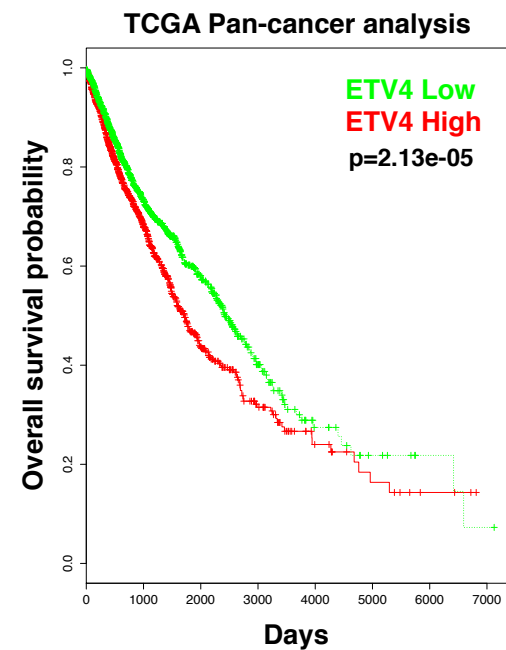
a**b****c**

Figure S15. ETV4 is broadly upregulated in tumors with CIC loss and correlates with worse survival in a pan-cancer analysis. (a) Schematic algorithm to identify differentially expressed CIC response genes in gastric adenocarcinoma tumors with genetic CIC loss and K-Ras mutant lung adenocarcinoma with functional CIC loss (b) Boxplots indicating median (gray bar) and interquartile range (box) of *ETV4* mRNA expression levels in the TCGA pan-cancer tumors with CIC copy number loss (n=82) or normal CIC (p=4.862e-08, n=2949). (c) Pan-cancer OS survival for patients with either *ETV4* high (n=1636) or *ETV4* low (n=1639) mRNA expression.

CIC mutations in Lung Adenocarcinoma

Lung Adenocarcinoma Dataset	Early Stage (I-II)	Advanced Stage (III-IV)
TCGA LUAD Provisional, 2016 (n = 488)	2/381 (0.5%)	3/107 (2.8%)
Rizvi et al. <i>Science</i> , 2015 (n = 34)	NA	2/34 (5.9%)
Total (n = 522), <i>p</i>-value = 0.02	2/381 (0.5%)	5/141 (3.5%)

Lung Adenocarinoma Dataset	Case	CIC Mutation	Stage	PolyPhen-2 (score)
TCGA LUAD Provisional, 2016	TCGA-69-7980-01	E236*	IA	Nonsense
	TCGA-97-7547-01	S1409L	IB	Probably Damaging (1.0)
	TCGA-64-5779-01	V1189L	IIIA	Probably Damaging (0.99)
	TCGA-75-6214-01	E1405*	IIIA	Nonsense
	TCGA-86-8056-01	R1412L	IIIA	Probably Damaging (0.99)
Rizvi et al. <i>Science</i> , 2015	JB112852	V672D	IV	Probably Damaging (0.99)
	ZA6965	A206V	IV	Probably Damaging (0.99)

Table S1. Non-synonymous *CIC* mutations in the TCGA lung adenocarcinoma provisional and Rizvi et al. metastatic lung adenocarcinoma datasets.

Table S2. Top 1500 differentially expressed genes between H1975 M1 (*CIC* null) and H1975 M1 with reconstituted *CIC* expression.

Table S3a. Top 1000 differentially expressed genes between H1975 and H1975 M1 cells. Ranked by p-value. Fold change and log2 fold change are also provided. The table is provided as an Excel File.

Table S3b. Top 1000 differentially expressed genes between H1975 and H1975 M2 cells. Ranked by p-value. Fold change and log2 fold change are also provided. The table is provided as an Excel File.

Table S4. 267 putative *CIC* response genes.

Supplementary table: primer sequences

Target gene	Sequence	Catalog #	Type
shMMP24a	CCGGCTGGTTAAAGTCCTATGGCTACTCGAGTAGCCATAGGAC TTTAACCAAGTTTTTG	TRCN0000052245	shRNA
shMMP24b	CCGGCCTCAGCCTGTCACCTACTATCTCGAGATAGTAGGTGACAGGCTGAGTTTTTG	TRCN0000052247	shRNA
shCICa	CCGGCCTGGGCTCTTACCGCAAGAAGCTCGAGTCTTTCGGTAAGAGCCAGGTTTTT	TRCN0000018924	shRNA
shCICb	CCGGCTTAGTGTATTCCGGACAAGAAGCTCGAGTCTTGTCCGAATACCTAAGTTTTG	TRCN0000329967	shRNA
shCICc	CCGGCTTAGTGTATTCCGGACAAGAAGCTCGAGTCTTGTCCGAATACCTAAGTTTTT	TRCN0000018920	shRNA
Primer	Sequence	Catalog #	Type
CIC forward	5'-ACCATGATGATGCGTGAGTT-3'	N/A	Genomic DNA
CIC reverse	5'-CTTCTCCCGCTGCATTAAAC-3'	N/A	Genomic DNA
GAPDH forward	5'-CCACAGTCCATGCCATCACTGCC-3'	N/A	Genomic DNA
GAPDH reverse	5'-GAGCTTGACAAAAGTGGTCGTG-3'	N/A	Genomic DNA
ETV4 forward	5'-CGCATCAGACCAAGACCCGTGG -3'	N/A	ChIP-PCR
ETV4 reverse	5'-CCGGAGAGTCTGCCGGCTGG -3'	N/A	ChIP-PCR
ETV5 forward	5'-GTGCTTCACTGACTCAGCTAAG -3'	N/A	ChIP-PCR
ETV5 reverse	5'-GCCATTGGCCAATCAGCACAGG -3'	N/A	ChIP-PCR
MMP24 forward	5'- GACACGTGGTGTGGCCATTC-3'	N/A	ChIP-PCR
MMP24 reverse	5'-GTAGGGCTCTGGGCTACTTGG-3'	N/A	ChIP-PCR
EGFR exon 21 forward	5'-TGACCCTGAATTCGGATGCA-3'	N/A	Genomic DNA
EGFR exon 21 reverse	5'-ATACAGCTAGTGGGAAGGCA-3'	N/A	Genomic DNA
Primer	Sequence	Catalog #	Type
G107E, G to A at 320	F: 5'-ctgagagccagaccgaccccc-3'	N/A	Mutagenesis
G107E, G to A at 320	R: 5'-gggggtccgggttctggctctcag-3'	N/A	Mutagenesis
R181W, C to T at 541	F: 5'-gaagatgagtcctcctctgggtaggcact-3'	N/A	Mutagenesis
R181W, C to T at 541	R: 5'-agtccctaccacaggaatgggactcatcttc-3'	N/A	Mutagenesis
Q247R, A to G at 740	5'-gcccaaggagaagcggaggtaccacgacc-3'	N/A	Mutagenesis
Q247R, A to G at 740	5'-ggctcgtggtactcctcctctctggc-3'	N/A	Mutagenesis
A281S, G to T at 841	5'-ggctcgtggctgctctctgagctggact-3'	N/A	Mutagenesis
A281S, G to T at 841	5'-agtccagctcagagagcaagccacgagcc-3'	N/A	Mutagenesis
S649F, C to T at 1946	5'-cggggcgaaggcactctggctc-3'	N/A	Mutagenesis
S649F, C to T at 1946	5'-gagccagagtgcctctgcccccg-3'	N/A	Mutagenesis
R666C, C to T at 1996	5'-ggcggcaggacagcagggggag-3'	N/A	Mutagenesis
R666C, C to T at 1996	5'-ctccccctgctctctgccc-3'	N/A	Mutagenesis
P722L, C to T at 2165	5'-ctgacaccagcagggagccccag-3'	N/A	Mutagenesis
P722L, C to T at 2165	5'-ctggggctccctcctggtgtcag-3'	N/A	Mutagenesis
G1098D, G to A at 3293	5'-gtgggtgcaggctctcagagtaaatgctgta-3'	N/A	Mutagenesis
G1098D, G to A at 3293	5'-taacagcattttactctgacagccctgcaccac-3'	N/A	Mutagenesis
A1185T, G to A at 3553	F: 5'-cacgggaatgctggtgatggctcctca-3'	N/A	Mutagenesis
A1185T, G to A at 3553	R: 5'-tgaaggcagccatcaccagctccctg-3'	N/A	Mutagenesis
R1515H, G to A at 4544	5'-ctgcatgctctctggtcacctcagcatctt-3'	N/A	Mutagenesis
R1515H, G to A at 4544	5'-aagatccgtgaggtgcaccagaagatcagcag-3'	N/A	Mutagenesis
Q1516H, G to T at 4548	5'-gcctgcatgcttatggccacctcagc-3'	N/A	Mutagenesis
Q1516H, G to T at 4548	5'-cgtgaggtgcgccataagatcagaggc-3'	N/A	Mutagenesis